nature physics

LETTERS

PUBLISHED ONLINE: 8 FEBRUARY 2009 | DOI: 10.1038/NPHYS1199

Preparation of non-local superpositions of quasi-classical light states

Alexei Ourjoumtsev*†, Franck Ferreyrol, Rosa Tualle-Brouri and Philippe Grangier

'Schrödinger cat' states of light[1], defined as quantum superpositions of quasi-classical coherent states, have recently emerged as an alternative to single-photon qubits for quantum-information processing[2–6]. Their richer structure provides significant advantages for quantum teleportation, universal quantum computation, high-precision measurements and fundamental tests of quantum physics[7–13]. Local superpositions of free-propagating coherent states have been realized experimentally, but their applications were so far limited by their extreme sensitivity to losses, and by the lack of quantum gates for coherent qubit rotations. Here, we demonstrate a simple approach to generating strongly entangled non-local superpositions of coherent states, using a very lossy quantum channel. Such superpositions should be useful for implementing coherent qubit-rotation gates, and for teleporting these qubits over long distances. The generation scheme may be extended to creating entangled coherent superpositions with arbitrarily large amplitudes.

Single-mode cat states can be considered as classical light waves with two opposite phases simultaneously, expressed as $\mathcal{C}(|\alpha\rangle + e^{i\phi}|-\alpha\rangle)$, where $|\alpha\rangle$ is a coherent state containing $|\alpha|^2$ photons on average and $\mathcal{C}$ is a normalization factor omitted in the following. The non-classical nature of such states appears most strikingly in the quantum statistics of the electric field: its quasi-probability distribution, called the Wigner function, presents quantum oscillations with negative values between the two classical states. The Wigner function $W(x,p)$, where $\hat{x} = (1/\sqrt{2})(\hat{a}+\hat{a}^\dagger)$ and $\hat{p} = (1/i\sqrt{2})(\hat{a}-\hat{a}^\dagger)$ are the quadrature operators of the quantized electric field, can be reconstructed by homodyne tomography[14] from several marginal distributions $P_\theta(x_\theta = x\cos\theta + p\sin\theta)$.

Besides their fundamental interest, arbitrary coherent superpositions $a|\alpha\rangle + b|-\alpha\rangle$ can be used as qubits carrying quantum information, if $|\alpha\rangle$ and $|-\alpha\rangle$ are sufficiently distinguishable ($|\alpha|^2 \gtrsim 2$). They present many advantages compared with discrete-variable qubits $a|0\rangle + b|1\rangle$, enabling one to circumvent the fundamental limits of discrete-variable quantum teleportation[7,15] or to carry out loophole-free Bell tests[13].

So far, their applications suffered from two major issues. One was the difficulty to build associated logic gates: arbitrary qubit rotations were believed to require either unrealistically strong nonlinear interactions, or very resource-consuming repeated infinitesimal rotations[8,13]. The other was more fundamental: the complex structure of these states, while offering many benefits, makes them notoriously fragile. For instance, many quantum-information processing (QIP) tasks require entangled cat states such as $|\psi_0\rangle = |\alpha\rangle_1|-\alpha\rangle_2 - |-\alpha\rangle_1|\alpha\rangle_2$. Theoretically, they can be obtained by splitting a single-mode cat $|\sqrt{2}\alpha\rangle - |-\sqrt{2}\alpha\rangle$ on a 50/50 beamsplitter and sending the two output modes to distant sites. But

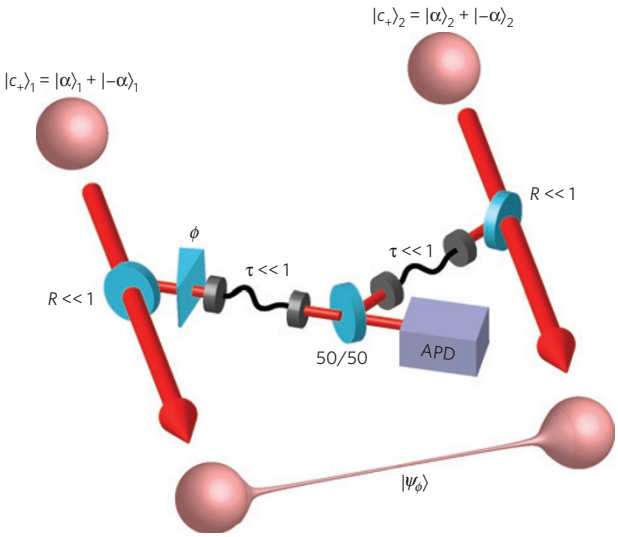

Figure 1 | Remote entanglement of two independent cat states $|c_+\rangle_{1,2}$ through lossy channels. The entanglement is created by non-local photon subtraction, by interfering small fractions R of each pulse, phase-shifted by ϕ, on a 50/50 beamsplitter. Then an APD photon detection in one of the outputs prepares the entangled state $|\psi_\phi\rangle$ (equation (1)), useful as a resource for long-distance quantum teleportation and phase-space rotations of coherent qubits (see text for details).

even small losses ϵ decrease the fidelity with the pure state as $-\epsilon|\alpha|^2$: transmitting cats with a large 'size' $|\alpha|^2$ becomes increasingly difficult. When $\epsilon > 1/2$ (that is, at ~15 km of optical fibre), the negativity of the Wigner function, and hence the quantum character of the state, disappears.

The approach demonstrated here circumvents the fragility of these states, typically described with continuous quadrature variables, by using the robustness offered by discrete-variable QIP. It consists of probabilistic entanglement swapping, similar to the protocol proposed by Duan, Lukin, Cirac and Zoller for discrete variables[16], where losses decrease the success rate instead of the state quality. We create long-range entanglement by subtracting a delocalized single photon from initially separable states, which can be manipulated locally and remain protected from losses. We show that the success rate and the quality of the prepared states are in principle independent of their size $|\alpha|^2$. In addition to long-distance quantum teleportation, they can be used to rotate a coherent qubit by an arbitrary angle with a simple photon counting measurement.

The protocol is illustrated in Fig. 1. Two single-mode cat states $|c_+\rangle_{1,2} = |\alpha\rangle_{1,2} + |-\alpha\rangle_{1,2}$ are prepared locally on two distant sites 1

Laboratoire Charles Fabry de l'Institut d'Optique, CNRS, Univ. Paris Sud, RD128, 91127 Palaiseau, France. *Present address: Max Planck Institut für Quantenoptik, Hans-Kopfermann-Straße 1, D-85748 Garching, Germany. †e-mail: alexei.ourjoumtsev@institutoptique.fr.

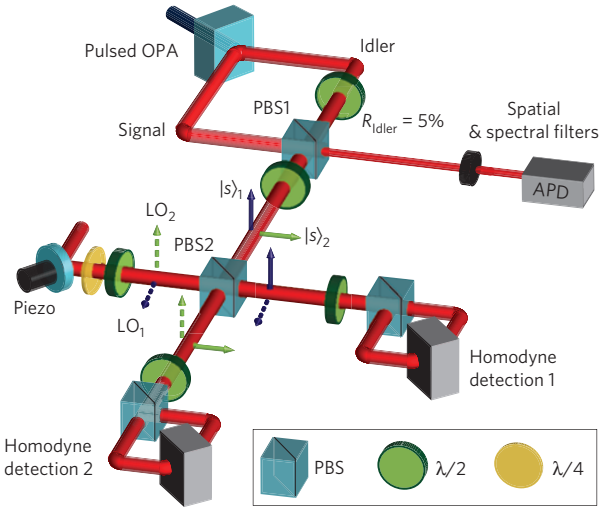

Figure 2 | Experimental set-up. The signal and idler from a pulsed OPA are recombined on a polarizing beamsplitter PBS1 to produce two independent squeezed light pulses $|s\rangle_1$ and $|s\rangle_2$, and the other channel of PBS1 is used as the conditioning channel to entangle them. The two entangled beams, co-propagating with orthogonal polarizations, are separated and mixed with two local oscillators LO_1 and LO_2 on PBS2, and finally detected by two independent homodyne detections.

and 2. A small fraction of each is reflected and sent through the lossy quantum link on a 50/50 beamsplitter. One of the subtracted beams is dephased by ϕ before interfering, and one of the beamsplitter outputs is monitored with a single-photon detector (avalanche photodiode, APD). A detection event heralds the subtraction of a single photon delocalized between the two modes 1 and 2 (ref. 17), applying the annihilation operator $\hat{a}_1 - e^{i\phi}\hat{a}_2$. As $\hat{a}(|\alpha\rangle \pm |-\alpha\rangle) = |\alpha\rangle \mp |-\alpha\rangle$, we prepare the strongly entangled coherent superposition

$$|\psi_\phi\rangle = -i\sin\frac{\phi}{2}|\alpha\rangle_1|\alpha\rangle_2 - \cos\frac{\phi}{2}|-\alpha\rangle_1|\alpha\rangle_2 + \cos\frac{\phi}{2}|\alpha\rangle_1|-\alpha\rangle_2 + i\sin\frac{\phi}{2}|-\alpha\rangle_1|-\alpha\rangle_2 \quad (1)$$

The generated state is essentially unaffected by the losses in the quantum channel, as long as the success rate exceeds the APD dark counts (as shown below, this is true even for long distances). For $\phi = 0$, this is the 'coherent Bell state' $|\psi_0\rangle$ above, proposed as a resource to teleport coherent qubits $|\xi\rangle = a|\alpha\rangle + b|-\alpha\rangle$ (refs 7,18). This can be done by mixing $|\xi\rangle$ with mode 1 on a 50/50 beamsplitter and counting photons in the output ports. Mode 2 is thus projected into $|\xi\rangle$, with the usual bit- and phase-flips depending on which combination of numbers (0, even), (0, odd), (even, 0) or (odd, 0) has been measured. The outcome (0, 0), corresponding to a failure, occurs with a probability $\sim e^{-2|\alpha|^2}$ and rapidly becomes negligible.

The crucial advantage of the states $|\psi_\phi\rangle$ prepared here appears for $\phi \neq 0$. In this case the teleportation also rotates the qubit by ϕ around the x axis of the Bloch sphere, transforming $|\xi\rangle$ into

$$|\xi'\rangle = [\cos\frac{\phi}{2}a - i\sin\frac{\phi}{2}b]|\alpha\rangle + [\cos\frac{\phi}{2}b - i\sin\frac{\phi}{2}a]|-\alpha\rangle$$

Such rotations, so far considered out of experimental reach, are essential for quantum computations and Bell tests.

Implementing this protocol experimentally requires two small independent 'Schrödinger kittens' $|c_+\rangle_{1,2}$ (see Fig. 1). For $|\alpha|^2 \lesssim 1$, they can be approximated by two squeezed vacuum states $|s\rangle_{1,2}$, which can be conveniently produced by recombining the two

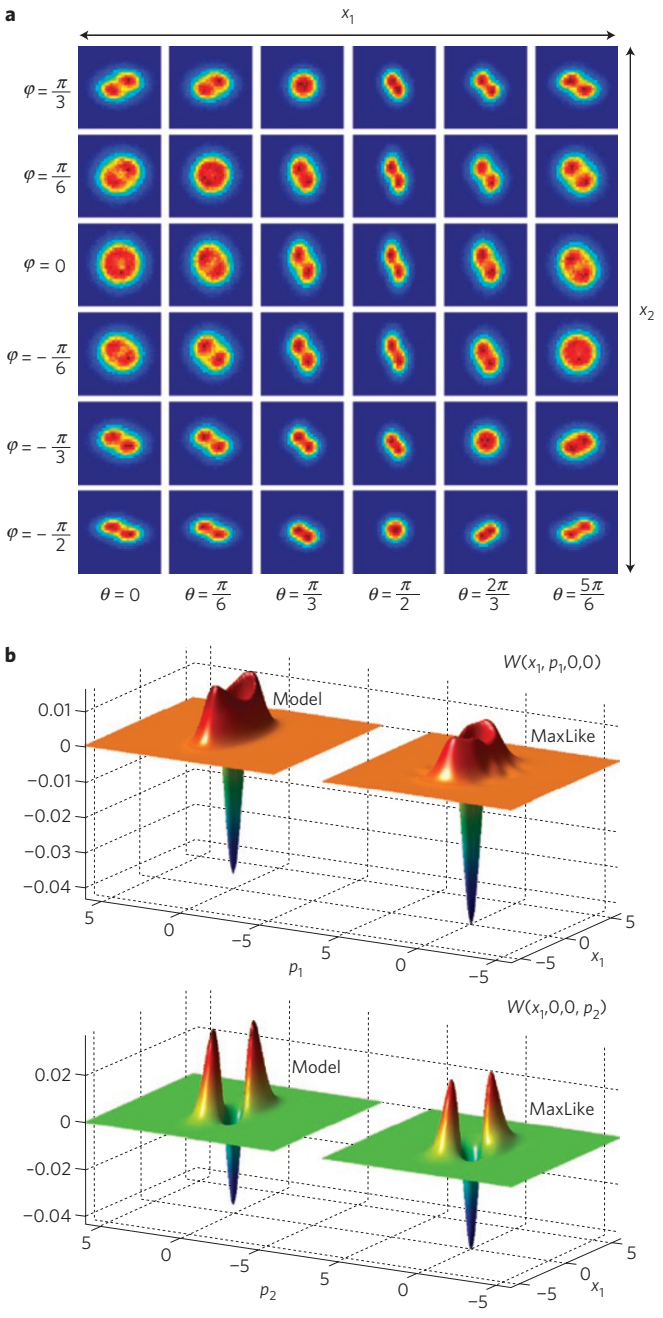

Figure 3 | Measured joint probability distributions and reconstructed Wigner functions. a, Experimentally measured two-mode quadrature distributions $P_{\theta,\varphi}(x_1, x_2)$, for six values of each angle θ and φ. **b**, Two 'cuts' of the experimentally reconstructed Wigner function of the generated state (corrected for homodyne losses), compared with the prediction of our analytical model (see Supplementary Information).

beams emitted by an optical parametric amplifier (OPA; Fig. 2). Recombining these beams on a polarization beamsplitter (PBS1) enables us to simultaneously tap the conditioning channel for coherent photon subtraction, with a phase $\phi = \pi/2$ to produce ancillas for teleporting Hadamard gates. The two orthogonally polarized co-propagating modes of the prepared state are separated on PBS2 and analysed with two independent homodyne detections.

Our OPA, described elsewhere[19], generates pairs of quadrature-entangled 150 fs pulses with a 780 kHz rate, with a gain $g = \cosh^2(r_0) = 1.18$ corresponding to 3.6 dB of two-mode squeezing. The signal and idler beams are superimposed on PBS1,

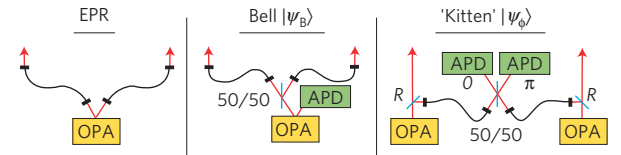

	$\mathcal{N}$	n_s (kHz)	$\mathcal{N}$	n_s (kHz)	$\mathcal{N}$	n_s (kHz)
A	0.64	780	0.31	120	0.43	13
B	0.03	780	0.003	120	0.43	1.4
C	0.03	780	0.003	58	0.40	0.65
D	0.03	780	0.002	12	0.15	0.14

Figure 4 | Estimated entanglement $\mathcal{N}$ and generation rate n_s for various quantum states. The state $|\psi_\phi\rangle$ obtained by non-local photon subtraction is compared with the direct transmission of two common entangled states generated with our set-up: the initial EPR state and the Bell state $|\psi_B\rangle$. We sequentially add various imperfections (see text for details), assuming (A) 780 kHz OPA repetition rate, 3.6 dB squeezing and $R = 5\%$, (B) 10 dB losses in each arm, (C) APDs with $n_d = 10$ Hz dark counts and $\eta_D = 45\%$ quantum efficiency, (D) broadband OPAs with $h = 1.02$, $\tau_f = 0.15$ and $\xi_f = 0.9$. With respect to the present experimental results, the quoted $\mathcal{N}$ (third column) is the observed one, whereas the success rate n_s has been doubled by detecting photons in the other port of the 50/50 beamsplitter, and shifting by π the phase of the second mode to obtain the same state $|\psi\rangle$.

so that $R = 5\%$ of the idler is sent into an APD counter through spatial and spectral filters. The light exiting through the other port is polarization-rotated by 45° and split on PBS2 to produce two independent squeezed vacuum pulses $|s\rangle_{1,2}$, superimposed with two local oscillators $LO_{1,2}$ (Fig. 2). The APD counts heralded single-photon subtractions from the idler, carrying out the non-local photon annihilation $\hat{a}_1 - i\hat{a}_2$ in the two squeezed pulses. This prepares the desired states with a rate $n_s \approx 600$ Hz, well above the APD dark counts ($n_d \approx 10$ Hz).

Complete two-mode tomography was carried out with two homodyne detections measuring two quadratures $x_1(\theta)$ and $x_2(\varphi)$, phase-controlled with waveplates and a piezo-mounted mirror. We measured 36 two-mode quadrature distributions $P_{\theta,\varphi}(x_1, x_2)$, each containing ≈160,000 data points divided in 40×40 bin histograms (Fig. 3). From these distributions, using a numerical maximal likelihood (MaxLike) algorithm[20] and correcting for a finite homodyne efficiency $\eta = 70\%$, we reconstructed the density matrix $\hat{\rho}$ and the two-mode Wigner function W of the generated state. Several 'cuts' of this function are presented in Fig. 3. The value at the origin (close to 0 without correction) is clearly negative: $W(0) = -0.04 \pm 0.01$ (ideally $W(0) = \pi^{-2} \approx -0.10$). This state has a fidelity $\mathcal{F} = 64 \pm 5\%$ with a pure state $|\psi_\phi\rangle$ described by $|\alpha|^2 = 0.65$ and $\phi = \pi/2$. It is mixed mostly with the non-conditioned squeezed vacuum ($\mathcal{F}_{sq} = 23 \pm 3\%$) by inconclusive APD detections. The entanglement is determined by the negativity[21] $\mathcal{N} = [||\hat{\rho}^{T_1}||_1 - 1]/2 = 0.25 \pm 0.04$ (ideally $\mathcal{N} = 0.5$). We developed a detailed analytical model (see Supplementary Information) in excellent agreement with the experiment, both with and without correction for losses.

The imperfections of the generated state are actually not attributed to the photon subtraction process, which is carried out with reflectivity $R = 5\%$, APD efficiency $\eta_D = 45\%$ and 10 Hz dark counts, but rather to the broad OPA parametric fluorescence. The excess noise in the analysed mode can be described by a phase-independent amplification of the initial squeezed vacuum, with a gain $h = 1.02$ (while $g = 1.18$; ref. 17). It also creates noise in other modes, resulting in unwanted APD triggers: despite tight filtering (transmission $\tau_f = 15\%$), the probability for a detected photon to come from the desired mode is $\xi_f = 0.90$. For instance, pure squeezed states ($h = 1$) would yield $\mathcal{N} = 0.48$ and a 98% fidelity with $|\psi_\phi\rangle$, despite all other imperfections. Therefore, the quality of the state is mainly limited by the specifics of our OPA, and not by the photon subtraction process.

An essential feature of this experiment is that the entanglement entirely results from the non-local photon subtraction: as expected, the tomography of the unconditioned state reveals two independent squeezed vacuum pulses with $\mathcal{N}_0 < 10^{-4} \approx 0$. The overall efficiency of the APD quantum channel used for this operation is $\tau = \eta_D \tau_f = 7\%$, which corresponds to 60 km of optical fibre at telecom wavelength, that is, to two sites separated by $2 \times 60 = 120$ km. The main contribution to these losses actually comes from the filters ($\tau_f = 15\%$), but even considering them as an intrinsic defect and adding an extra 10 dB losses (2×50 km) would still yield $\mathcal{N} \approx 0.15$. In comparison, the same state prepared locally and sent through this fibre would arrive with only $\mathcal{N} \approx 10^{-3}$.

In terms of entanglement as such, one can compare these states to others generated with the same tools. We realized a comparative experiment by sending all of the idler light to the APD, conditionally preparing single photons in the signal mode, and splitting them on a 50/50 beamsplitter between the two homodyne detections (as in ref. 22). The resulting state $|\psi_B\rangle = ((|1\rangle_1|0\rangle_2 - |0\rangle_1|1\rangle_2)/\sqrt{2})$, ideally presenting the same entanglement, was generated 20 times faster, but even without losses its entanglement was slightly lower ($\mathcal{N} = 0.19 \pm 0.02$), owing to higher photon number contributions. Sharing this state through two 50 km fibres would yield again $\mathcal{N} \approx 10^{-3}$. For the initial Einstein–Podolsky–Rosen (EPR) state, $\mathcal{N}$ would drop from 0.64 to 0.03 (Fig. 4), showing that our protocol is efficient for entanglement distribution in general.

The size of the prepared kittens, although relatively small ($|\alpha|^2 = 0.65$), is almost sufficient for the Bell test described in ref. 13 ($|\alpha|^2 \geq 0.71$). It can be increased by using larger initial cat states $|c_+\rangle_{1,2}$, which can be generated with the same experimental tools[5,6]. For a larger initial cats size $|\alpha|^2$, one should reduce the tapped fraction R, keeping the product $R|\alpha|^2$ constant: the fidelity and speed of the protocol are then unchanged.

This scheme overcomes, to some extent, the high sensitivity to losses encountered in many continuous-variable QIP protocols, which do not easily allow one to postselect successful events. By using the specific discrete-variable advantage of discarding those events where photons were lost, we have shown that sophisticated continuous-variable entangled resources can be prepared despite strong losses in quantum channels. These states may be used as ancillas to implement arbitrary controlled qubit rotations, required in most QIP protocols, without needing strong nonlinearities or extensive experimental resources.

Received 10 June 2008; accepted 7 January 2009; published online 8 February 2009

References

1. Schrödinger, E. Die gegenwärtige Situation in der Quantenmechanik. *Naturwissenschaften* **23**, 807–812 (1935).
2. Ourjoumtsev, A., Tualle-Brouri, R., Laurat, J. & Grangier, P. Generating optical Schrödinger kittens for quantum information processing. *Science* **312**, 83–86 (2006).
3. Neergaard-Nielsen, J. S., Nielsen, B. M., Hettich, C., Mølmer, K. & Polzik, E. S. Generation of a superposition of odd photon number states for quantum information networks. *Phys. Rev. Lett.* **97**, 083604 (2006).
4. Wakui, K., Takahashi, H., Furusawa, A. & Sasaki, M. Controllable generation of highly nonclassical states from nearly pure squeezed vacua. *Opt. Express* **15**, 3568–3574 (2007).
5. Ourjoumtsev, A., Jeong, H., Tualle-Brouri, R. & Grangier, P. Generation of optical Schrödinger cats from photon number states. *Nature* **448**, 784–786 (2007).
6. Takahashi, H. *et al.* Generation of large-amplitude coherent-state superposition via ancilla-assisted photon-subtraction. *Phys. Rev. Lett.* **101**, 233605 (2008).
7. Jeong, H., Kim, M. S. & Lee, J. Quantum-information processing for a coherent superposition state via a mixed entangled coherent channel. *Phys. Rev. A* **64**, 052308 (2001).

8. Ralph, T. C., Gilchrist, A., Milburn, G. J., Munro, W. J. & Glancy, S. Quantum computation with optical coherent states. *Phys. Rev. A* **68**, 042319 (2003).
9. Munro, W. J., Nemoto, K., Milburn, G. J. & Braunstein, S. L. Weak-force detection with superposed coherent states. *Phys. Rev. A* **66**, 023819 (2002).
10. Toscano, F., Dalvit, D. A. R., Davidovich, L. & Zurek, W. H. Sub-Planck phase-space structures and Heisenberg-limited measurements. *Phys. Rev. A* **73**, 023803 (2006).
11. Wenger, J., Hafezi, M., Grosshans, F., Tualle-Brouri, R. & Grangier, P. Maximal violation of Bell inequalities using continuous-variable measurements. *Phys. Rev. A* **67**, 012105 (2003).
12. Haroche, S. *Science and Ultimate Reality* (Cambridge Univ. Press, 2004).
13. Stobińska, M., Jeong, H. & Ralph, T. C. Violation of Bell's inequality using classical measurements and non-linear local operations. *Phys. Rev. A* **75**, 052105 (2007).
14. Leonhardt, U. *Measuring the Quantum State of Light* (Cambridge Univ. Press, 1997).
15. Lütkenhaus, N., Calsamiglia, J. & Suominen, K. A. Bell measurements for teleportation. *Phys. Rev. A* **59**, 3295–3300 (1999).
16. Duan, L.-M., Lukin, M. D., Cirac, J. I. & Zoller, P. Long-distance quantum communication with atomic ensembles and linear optics. *Nature* **414**, 413–418 (2001).
17. Ourjoumtsev, A., Dantan, A., Tualle-Brouri, R. & Grangier, P. Increasing entanglement between Gaussian states by coherent photon subtraction. *Phys. Rev. Lett.* **98**, 030502 (2007).
18. Enk, S. J. V. & Hirota, O. Entangled coherent states: Teleportation and decoherence. *Phys. Rev. A* **64**, 022313 (2001).
19. Wenger, J., Ourjoumtsev, A., Tualle-Brouri, R. & Grangier, P. Time-resolved homodyne characterization of individual quadrature-entangled pulses. *Eur. Phys. J. D* **32**, 391–396 (2005).
20. Lvovsky, A. I. Iterative maximum-likelihood reconstruction in quantum homodyne tomography. *J. Opt. B* **6**, S556–S559 (2004).
21. Vidal, G. & Werner, R. F. A computable measurement of entanglement. *Phys. Rev. A* **65**, 032314 (2002).
22. Babichev, S. A., Appel, J. & Lvovsky, A. I. Homodyne tomography characterization and nonlocality of a dual-mode optical qubit. *Phys.Rev. Lett.* **92**, 193601 (2004).

Acknowledgements

This work is supported by the EU ICT/FET program COMPAS.

Additional information

Supplementary Information accompanies this paper on www.nature.com/naturephysics. Reprints and permissions information is available online at http://npg.nature.com/reprintsandpermissions. Correspondence and requests for materials should be addressed to A.O.